

Synthesis and Characterization of Acetylene-Linked Bisphenalenyl and Metallic-Like Behavior in Its Charge-Transfer Complex

Takashi Kubo,^{*,[a]} Yuko Goto,^[a] Mikio Uruichi,^[b] Kyuya Yakushi,^[b] Masayoshi Nakano,^[c] Akira Fuyuhiko,^[a] Yasushi Morita,^{*,[a, d]} and Kazuhiro Nakasuji^{*,[a]}

Dedicated to Professor Ichiro Murata on the occasion of his 77th birthday

Abstract: We prepared and isolated a phenalenyl-based neutral hydrocarbon (**1b**) with a biradical index of 14%, as well as its charge-transfer (CT) complex **1b**-F₄-TCNQ. The crystal structure and the small HOMO-LUMO gap assessed by electrochemical and optical methods support the singlet-biradical contribution to the ground state of the neutral **1b**. This biradical character suggests that **1b** has the electronic structure of phenalenyl radicals coupled weakly through an acetylene linker, that is, some independence of

the two phenalenyl moieties. The monocationic species **1b**^{•+} was obtained by reaction with the organic electron acceptor F₄-TCNQ. The cationic species has a small disproportionation energy ΔE for the reaction $2 \times \mathbf{1b}^{\bullet+} \rightleftharpoons \mathbf{1b} + \mathbf{1b}^{2+}$, which presumably originates from the independence of the phenalenyl moieties. The small ΔE

led to a small on-site Coulombic repulsion $U_{\text{eff}} = 0.61$ eV in the CT complex. Moreover, a very effective orbital overlap of the phenalenyl rings between molecules afforded a relatively large transfer integral $t = 0.09$ eV. The small $U_{\text{eff}}/4t$ ratio (=1.7) resulted in a metallic-like conductive behavior at around room temperature. Below 280 K, the CT complex showed a transition into a semiconductive state as a result of bond formation between phenalenyl and F₄-TCNQ carbon atoms.


Keywords: acetylene • charge transfer • phenalenyl • radical ions • radicals

[a] Prof. T. Kubo, Y. Goto, Dr. A. Fuyuhiko, Prof. Y. Morita, Prof. K. Nakasuji
Department of Chemistry
Graduate School of Science, Osaka University
Machikaneyama 1-1, Toyonaka
Osaka 560-0043 (Japan)
Fax: (+81)6-6850-5387
E-mail: kubo@chem.sci.osaka-u.ac.jp
morita@chem.sci.osaka-u.ac.jp
nakasuji@chem.sci.osaka-u.ac.jp

[b] Dr. M. Uruichi, Prof. K. Yakushi
Department of Applied Molecular Science
Institute for Molecular Science
Okazaki 444-8585 (Japan)

[c] Prof. M. Nakano
Department of Materials Engineering Science
Graduate School of Engineering Science
Osaka University
Machikaneyama 1-3, Toyonaka
Osaka 560-8531 (Japan)

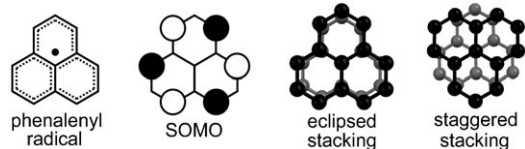
[d] Prof. Y. Morita
PRESTO
Japan Science and Technology Agency (JST)
Saitama 332-0012 (Japan)

 Supporting information for this article is available on the WWW under <http://www.chemasia.org> or from the author.

Introduction

One of the remarkable functional properties of π -conjugated organic molecules is their electrical conductivity, for which the on-site Coulombic repulsion U and the transfer integral t are crucial factors.^[1] Significant effort has been devoted to molecular designs toward a small U and a large t value, including expansion of the π -system, introduction of chalcogen atoms, and so on.^[2] Recent extensive studies on phenalenyl-based molecular conductors, whose features of electronic structure are associated with a spiroconjugative interaction of phenalenyl radical and cation, revealed that phenalenyl would be a promising structure for highly conductive materials as a result of its low $U/4t$ ratio,^[3] which originates from two characteristics of the phenalenyl radical.^[4,5] First, this radical has a singly occupied molecular orbital (SOMO) with nonbonding character; consequently, addition and removal of an electron should not affect the π -bonding energy of the system within the simple Hückel molecular-orbital theory. The parent phenalenyl radical shows a relatively small difference between the first oxidation and first reduction potentials ($\Delta E^{\text{redox}} = 1.6$ V).^[6] A small ΔE^{redox}

is a good indicator of a small U value, although ΔE^{redox} and U are solution-phase (i.e., single-molecule) and solid-state (i.e., molecular-aggregate) properties, respectively.^[1,7] Second, the sixfold symmetry of the SOMO gives perfect orbital overlap in both eclipsed and staggered stacking motifs, the latter of which is seen in 2,5,8-tri-*tert*-butylphenalenyl radical,^[8] thus leading to a large t value.



Recently, we demonstrated that some phenalenyl-based closed-shell polycyclic hydrocarbons have singlet-biradical character, in which the bis(phenalenyl radical) canonical form largely contributes to the electronic structure in the ground state.^[9] Although singlet biradicals, whose features of electronic structure are derived from a weak coupling of two radical centers, are generally highly reactive species that give dimeric or polymeric compounds,^[10] the bisphenalenyl singlet biradicals can be isolated in air by utilizing the spin-delocalizing character of the phenalenyl radical. The most important feature of the singlet biradicals isolated is the substantially short π - π overlap of the phenalenyl rings in the staggered stacking.^[9b] This favorable stacking gives a large orbital overlap between molecules; thus, large bandwidths $W (=4t)$ are achieved in the valence and conduction bands.^[11]

The staggered stacking of the phenalenyl system would not be limited to the radical pair, according to Kochi and co-workers.^[12] They demonstrated that a phenalenyl radical and cation pair also forms the dimeric staggered stacking in solution. The spirobiphenalenyl system of Haddon and co-workers would be a good representative for the staggered stacking based on a radical-cation pair in the solid state.^[3b] In the case of our bisphenalenyl system, monocationic species of the singlet biradicals would have phenalenyl radical and cation electronic structure, and a large orbital overlap

Abstract in Japanese:

我々はフェナレニルを基盤とする炭化水素分子 **1b** とその電荷移動錯体を合成、単離した。**1b** は量子化学計算から 14%の一重項ビラジカル性を有していると予想される。実験的に見積もった小さな HOMO-LUMO ギャップや結晶構造から、**1b** の基底状態にはビラジカル構造の寄与があることがわかり、二つのフェナレニル部位は弱い相互作用、すなわちある程度の独立性を有することが明らかとなった。**1b** の一電子酸化種はフェナレニル部位の独立性のため不均化エネルギー ΔE が小さく、そのため **1b** と $F_4\text{-TCNQ}$ から成る電荷移動錯体 (イオン化度 = 1) は、小さなオンサイトクーロン反発エネルギー U を有していた。加えて結晶中におけるフェナレニル環同士の軌道の大きな重なりにより、大きな移動積分 t も有していた。結果的に電荷移動錯体は $U/4t$ が小さくなり、そのため室温付近で金属的な挙動を示した。これらの結果は、フェナレニルを基盤とする一重項ビラジカルの一電子酸化種が導電体の優れた構成成分と成り得ることを示唆するものである。一方、280 K 以下では半導体相への転移が確認されたが、これはフェナレニルと $F_4\text{-TCNQ}$ の一部の炭素原子同士が σ 結合を形成するためであることが、X線構造解析により明らかとなった。

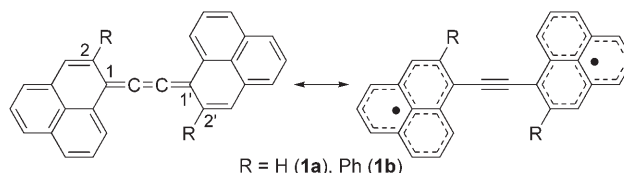
between molecules is expected as in the case of the neutral singlet biradicals and the spirobiphenalenyl system.

To obtain further insight into the solid-state properties of bisphenalenyl compounds, we focused on hydrocarbon **1a** (Scheme 1), which was isolated as an unstable crystalline solid and investigated with regard to its solution-based amphoteric redox property.^[13] Herein, we describe the synthesis, isolation, and characterization of phenyl derivative **1b** and assess its biradical character by structural analysis, electronic spectroscopy, and cyclic voltammetry. Furthermore, we report the generation and solid-state properties of the monocationic species of **1b**, which is the chemistry of a singly oxidized state of a singlet biradical.

Results and Discussion

Theoretical Consideration of Biradical Character

The molecule **1a** consists of two phenalenyl radicals and an acetylene linker and resonates with a closed-shell form (Kekulé structure), as shown in Scheme 1. This singlet com-



Scheme 1. Resonance structures of **1**.

pound is designed so as to give low oxidation potentials and high reduction potentials. The molecular design strongly depends on the nonbonding character of the SOMO in phenalenyl radical. Under the guidance of the simple Hückel molecular-orbital theory, the nonbonding molecular orbital has an energy of α , whereas acetylene has well-separated frontier orbitals with energies of $\alpha \pm 1.4\beta$.^[14] According to the perturbation theory, a pair of nonbonding SOMOs (Ψ_p) in two phenalenyl radicals should be perturbed slightly by the frontier orbitals (Ψ_a) of acetylene because of a large absolute value of the denominator in the orbital-energy change given by $E = a^2 b^2 \beta^2 / [E(\Psi_p) - E(\Psi_a)]$, in which a and b are the atomic-orbital coefficients of Ψ_p and Ψ_a at the linked sites, respectively (see Supporting Information, Figure S1 for a correlation diagram of these molecular orbitals calculated with a more sophisticated method). This weak perturbation by the acetylene linker leads to a small HOMO-LUMO energy gap in **1a**, which retains the nonbonding character of phenalenyl radical. Figure 1a and b shows the HOMO and LUMO of **1a**.

The small energy gap and large spatial overlap between the HOMO and LUMO give a chance for strong mixing of the doubly excited configuration ${}^1\Phi_{\text{H,H} \rightarrow \text{L,L}}$ with the ground-state configuration ${}^1\Phi_{\text{H,H}}$. The biradical character can be estimated from the extent of the admixture, because the LUMO occupation number in a multiconfigurational wave-

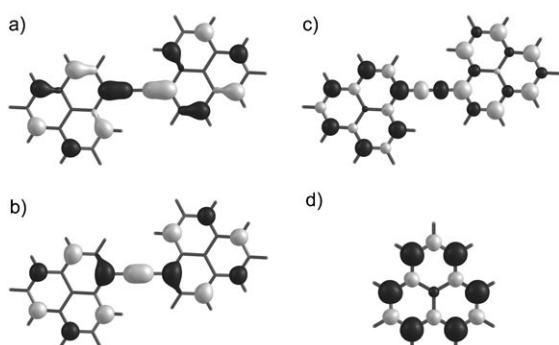


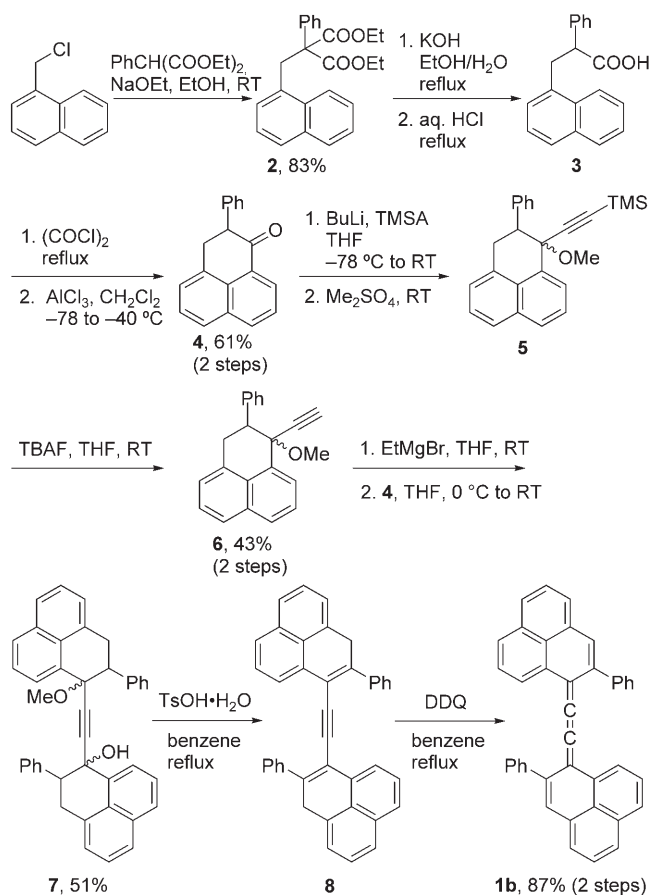
Figure 1. a) HOMO and b) LUMO of **1a** calculated with the RB3LYP/6-31G** method; dark- and light-gray surfaces represent the relative signs of the orbital coefficients. Spin densities of c) **1a** and d) phenalenyl radical calculated with the UB3LYP/6-31G** method; dark- and light-gray surfaces represent α and β spin densities drawn at the $0.004 \text{ e a.u.}^{-3}$ level, respectively.

function is a good indicator of singlet-biradical character.^[15] A perfect biradical is characterized by occupation numbers of 1.0 for the HOMO and LUMO (i.e., $y=100\%$), whereas a perfect closed-shell molecule has occupation numbers of 2.0 and 0.0 for the HOMO and LUMO (i.e., $y=0\%$), respectively.^[16] A CASSCF(2,2) calculation for **1a** gave HOMO and LUMO occupation numbers of 1.86 and 0.14, respectively. The biradical index y was determined to be 14% on the basis of the LUMO occupation number. Recent progress of unrestricted DFT calculations in the broken-symmetry formalism enables an approximate description of spin structure in singlet biradicals.^[17] A broken-symmetry UB3LYP calculation for **1a** showed a large spin density on the phenalenyl rings with the same distribution pattern as that of phenalenyl radical as shown in Figure 1c and d. Thus, the ground state of **1a** can be described by a resonance structure of Kekulé and biradical canonical forms (Scheme 1).

Synthesis of Phenyl Derivative **1b**

The reactive **1a** can be stabilized by substituents on the phenalenyl rings. Bulky substituents, however, prohibit effective π - π overlap between molecules in the solid state and decrease the electron–electron interaction between molecules. We decided to introduce phenyl groups on the 2- and 2'-positions of the rings, because it seemed unlikely that the phenyl groups would prohibit large π - π overlap, according to our study with the Corey–Pauling–Koltun (CPK) model. Furthermore, small coefficients of the frontier orbitals at these positions would not affect the electronic structure of the parent molecule (Figure 1).

The phenyl derivative **1b** was prepared according to the procedure shown in Scheme 2. The phenyl group was introduced by the reaction of 1-chloromethylnaphthalene with diethyl 2-phenylmalonate. After hydrolysis and decarboxylation of **2**, the resulting **3** was subjected to Friedel–Crafts cyclization to give dihydrophenalenone **4**. The reaction of **4** with lithium trimethylsilylacetylide followed by methylation



Scheme 2. Preparation of **1b**. DDQ=2,3-dichloro-5,6-dicyano-*p*-benzoquinone, TBAF=tetra-*n*-butylammonium fluoride, TMSA=trimethylsilylacetylene, Ts=*p*-toluenesulfonyl.

afforded **5** as a diastereomeric mixture. After deprotection of the TMS group, we obtained a diastereomer of **6** in pure form by recrystallization. The other diastereomer of **6** included some impurities, which could not be removed by conventional purification methods. The acetylide of the purified **6** was generated with EtMgBr and then treated with **4** to give **7** as a diastereomeric mixture. Dehydration and cleavage of propargyl ether in the mixture **7** with a catalytic amount of TsOH·H₂O afforded dihydro precursor **8** as an air-sensitive solid. The final target compound **1b** was obtained as dark-blue prisms by dehydrogenation of **8** with DDQ. In contrast to **1a**, the solid **1b** was found to be stable under atmospheric conditions for several weeks.

Determination of the HOMO–LUMO Gap of **1b**

As mentioned above, a small gap and a large spatial overlap between HOMO and LUMO are essential factors for biradical character. The HOMO–LUMO gap of **1b** was estimated by electrochemical and optical methods. The cyclic voltammogram (see Supporting Information, Figure S2) of **1b** gave two reversible oxidation ($E_1^{\text{ox}} = +0.05$, $E_2^{\text{ox}} = +0.42 \text{ V}$ vs. FcH/FcH⁺; FcH=ferrocene) and two reversible reduction waves ($E_1^{\text{red}} = -1.44$, $E_2^{\text{red}} = -1.79 \text{ V}$), which led to an elec-

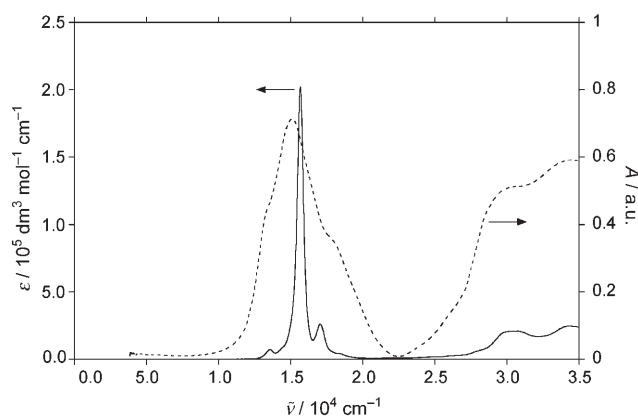


Figure 2. Optical-absorption spectra of **1b** in CH_2Cl_2 (solid line) and KBr pellet (dashed line).

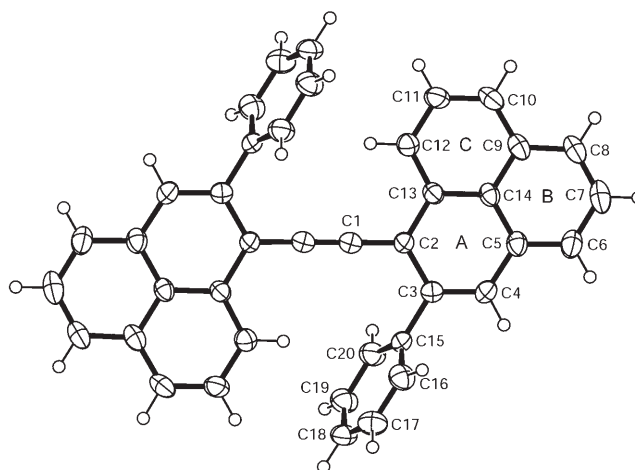


Figure 3. ORTEP drawing of **1b** with thermal ellipsoids at 50% probability.

trochemical HOMO–LUMO gap of 1.49 eV.^[18] The absorption spectrum of **1b** in CH_2Cl_2 (Figure 2) afforded an intense low-energy band at 15700 cm^{-1} (638 nm, $\epsilon = 202300\text{ cm}^{-1}\text{ mol}^{-1}\text{ L}$). An INDO/S calculation for **1a** predicted a fully allowed HOMO–LUMO transition at 16100 cm^{-1} (620 nm). Thus, the optical HOMO–LUMO energy gap was determined to be 1.94 eV. Although there is no decisive guideline on how small an energy gap is required for singlet-biradical character, the HOMO–LUMO gaps determined are sufficiently small according to the Hoffman suggestion that a gap of 1.5 eV is borderline for a triplet ground state.^[19] A small HOMO–LUMO gap is relevant to promotion to an energetically low-lying triplet excited state as well as singlet-biradical character. The $^1\text{H NMR}$ spectrum of **1b** showed signal line broadening for the protons on the phenalenyl rings above room temperature (see Supporting Information, Figure S3). This behavior might be caused by thermal excitation to the triplet state, although ESR signals typical for triplet species were not detected in a powdered sample of **1b** even at 400 K.^[20]

Crystal Structure of **1b**

Recrystallization of **1b** from a solution of toluene gave single crystals suitable for X-ray crystallography. As shown in Figure 3, **1b** has the *E* conformation with a parallel arrangement of the two phenalenyl rings.^[21] Strong bond alternation was observed on the A ring of the phenalenyl rings, especially for C13–C2 (1.460(3) Å), C2–C3 (1.441(4) Å), C3–C4 (1.367(4) Å), and C4–C5 (1.446(4) Å). The geometries of the B and C rings are similar to that of naphthalene (see Supporting Information, Figure S4).^[22] These geometrical considerations on the phenalenyl rings indicate the large contribution of the Kekulé structure to the ground state. In the cumulene moiety, however, the terminal (C1–C2 1.378(4) Å) and central (C1–C1' 1.234(5) Å) double bonds are longer and shorter than those of $\text{C}(\text{sp}^2)$ -substituted butatrienes (1.334–1.349 Å for the terminal and 1.24–1.260 Å for the central),^[23] respectively. More single- and triple-bond

character in the cumulene moieties suggests the biradical contribution in the ground state.

Unfortunately, there were no π – π contacts shorter than the sum of the van der Waals radii of the carbon atoms between molecules (Figure 4). The packing is dominated by

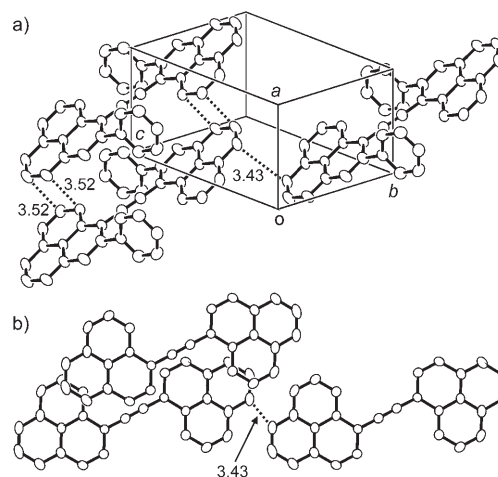
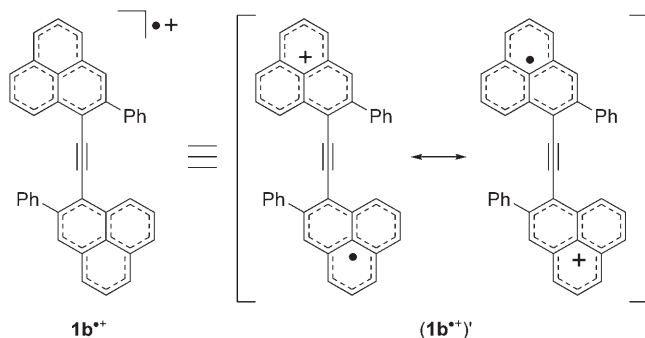


Figure 4. a) Crystal packing of **1b**. Hydrogen atoms are omitted for clarity. b) Overlap pattern of **1b**. Hydrogen atoms and phenyl groups are omitted for clarity.

$\text{CH}\cdots\pi$ interactions and is quite different from that of the polycyclic hydrocarbon with 30% biradical character mentioned in the Introduction,^[9b] which has large π – π overlap. The small biradical character does not afford effective intermolecular spin–spin interaction, and the $\text{CH}\cdots\pi$ interactions are stronger than the weak spin–spin interaction. The non-effective π – π overlap results in small band dispersions in all directions (not shown). The absorption spectra of powdered solid **1b** in a KBr pellet showed no appreciable lower-energy shift relative to the solution band (Figure 2), thus reflecting the small orbital overlap between molecules.

Generation of Radical Cation Species of **1b**

The small electrochemical gap is a characteristic of the singlet biradical **1b**. Another prominent feature is the small difference (ΔE) between the first and second oxidation (and reduction) potentials. The small ΔE value indicates that singly oxidized (and reduced) species of **1b** have a small disproportionation energy for the reaction $2 \times \mathbf{1b}^{+\cdot} \rightleftharpoons \mathbf{1b} + \mathbf{1b}^{2+}$. A small disproportionation energy is known to be an important factor for highly conductive materials.^[24] Compounds with weakly interacting radical centers are prone to small ΔE values;^[25] thus, $\mathbf{1b}^{+\cdot}$ and $\mathbf{1b}^{\cdot-}$ would be good candidates for electroconductive materials based on the one-electron redox species of weakly coupled electron systems. The reaction of **1b** with a slight excess (1.2 equiv) of tetrafluorotetracyanoquinodimethane (F_4 -TCNQ) gave shiny black crystals of a charge-transfer (CT) complex composed of **1b** and F_4 -TCNQ (1:1). The crystal was stable under atmospheric conditions for several weeks. The ionicity of the CT complex was estimated by using Raman spectroscopy, which showed a strong peak at 1643 cm^{-1} assignable to the $a_g \nu_2$ mode dominated by C=C stretching of the F_4 -TCNQ six-membered ring. The peak position is similar to that of the F_4 -TCNQ radical anion, which indicates complete charge transfer (i.e., ionicity=1).^[26] Therefore, **1b** can be safely assigned as a monoradical cation. The spin and charge of $\mathbf{1b}^{+\cdot}$ should delocalize over the entire molecule, thus retaining the nonbonding character of phenalenyl radical, according to the ESR measurement of $\mathbf{1a}^{+\cdot}$ previously reported.^[27] As shown in Scheme 3, the best description of the electronic structure of $\mathbf{1b}^{+\cdot}$ is the resonance of two canonical structures ($\mathbf{1b}^{+\cdot}$), in which phenalenyl radical and cation are connected through the acetylene conjugation.



Scheme 3. Resonance structures of $\mathbf{1b}^{+\cdot}$.

Crystal Structure and Conductive Behavior of CT Complex Around Room Temperature

X-ray crystallographic analysis of the CT complex revealed that $\mathbf{1b}^{+\cdot}$ has more acetylenic character in the linker moiety (terminal C1–C2 1.403(3) Å; central C1–C1' 1.211(4) Å).^[28] Moreover, the A ring (Figure 3) showed appreciable decrease in bond alternation relative to the neutral **1b** for the following bonds: C13–C2 1.444(3), C2–C3 1.422(3), C3–C4 1.371(3), C4–C5 1.422(3) Å. These geometric considerations

support the limiting structure ($\mathbf{1b}^{+\cdot}$) in Scheme 3 for the ground state of $\mathbf{1b}^{+\cdot}$. The most important feature in the crystal structure is the molecular packing of $\mathbf{1b}^{+\cdot}$, in which there is large π – π overlap of the phenalenyl rings with an average distance of 3.34 Å in the staggered stacking motif (Figure 5). The molecules are completely superimposed at

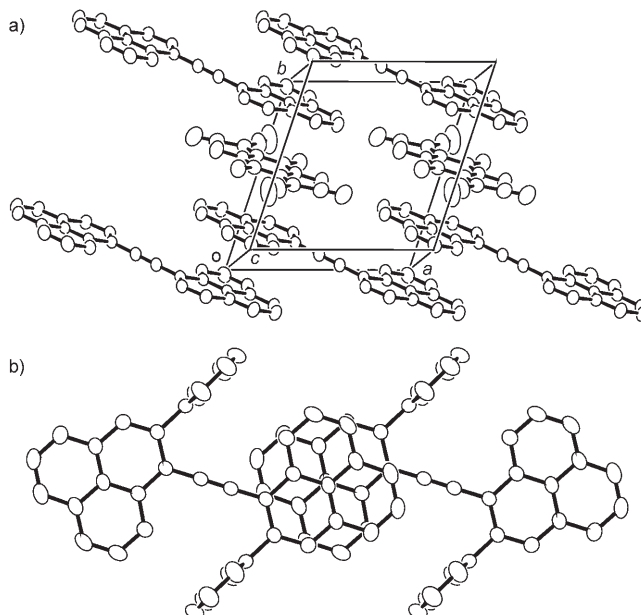


Figure 5. a) Crystal structure of the $\mathbf{1b}$ - F_4 -TCNQ CT complex at room temperature. Phenyl groups and hydrogen atoms are omitted for clarity. b) Overlap pattern of $\mathbf{1b}^{+\cdot}$. Hydrogen atoms are omitted for clarity.

the carbon positions that have large atomic-orbital coefficients in the SOMO of $\mathbf{1b}^{+\cdot}$, thus leading to very effective orbital overlap between molecules. The positive charge induced by the removal of one electron lowers the CH \cdots π interaction, which is one of the dominant factors for controlling the packing of the neutral **1b**. Besides, the attractive force between phenalenyl radical and cation moieties, which could be recognized as a bonding interaction similar to that in the “ π -pimer” studied thoroughly by Kochi and co-workers,^[12] would contribute to the characteristic overlap. The band-structure calculation with extended Hückel theory (EHT) gave a relatively large dispersion (0.42 eV) for a half-filled band along the π – π stacking direction, $X(\frac{1}{2}, 0, 0)$. The electroconductivity of the CT complex was measured by using four-probe contacts on a single crystal. The room-temperature (290 K) resistivity ρ_{RT} was about 0.7 $\Omega \text{ cm}$ with metallic-like behavior down to about 280 K (Figure 6). Semiconductive behavior at low temperature will be discussed below.

Solid-State Electronic Structure of CT Complex at Around Room Temperature

Figure 7 shows the optical conductivity σ_{opt} of the CT complex, which was obtained by Kramers–Kronig transformation of the reflection spectra of a single crystal. A broad

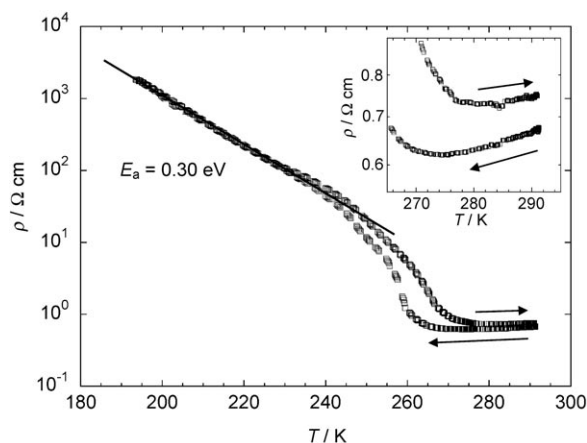


Figure 6. Single-crystal resistivity of **1b**-F₄-TCNQ as a function of temperature. Inset: Resistivity at around room temperature.

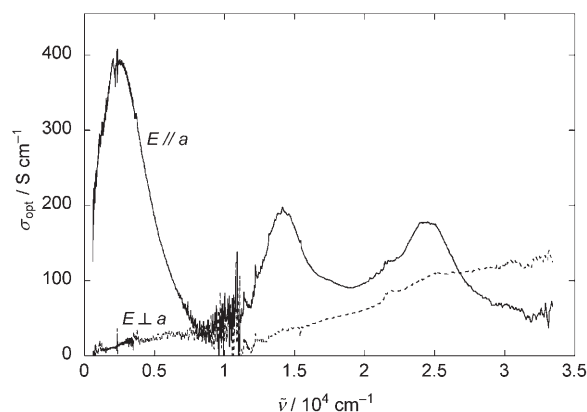


Figure 7. Optical conductivity σ_{opt} of **1b**-F₄-TCNQ at room temperature obtained with light polarized along (solid line) and perpendicular (dashed line) to the *a* axis on the single-crystal (001) face.

peak polarized along the *a* axis ($E//a$) was observed at 2600 cm^{-1} , whereas the $E\perp a$ spectrum gave a weak band below 13000 cm^{-1} . The low-energy broad peak ($E//a$) approached zero conductivity toward frequency $\omega=0$. This finding indicates a small energy gap between the valence and conduction bands, and, accordingly, the CT complex is intrinsically regarded as a Mott–Hubbard insulator. Analyzing the peak profile, we determined a transfer integral $t=0.09\text{ eV}$ and an effective on-site Coulombic repulsion $U_{\text{eff}}=0.61\text{ eV}$.^[29] The transfer integral determined gives a bandwidth $W (=4t)$ of 0.36 eV , which is consistent with the calculated dispersion of the half-filled band (0.42 eV) and is comparable to that of general highly conductive organic materials. The effective π – π overlap on the phenalenyl rings is responsible for the relatively large band dispersion. The biradical character of **1b** in the neutral state is in close relation to a weak interaction between the phenalenyl rings, thus leading to some independence of the redox centers. Hence, the first and second oxidation waves are close in potential, and the small U_{eff} value is established in the CT complex.^[30] The

small $U_{\text{eff}}/4t$ ratio ($=1.7$) is relevant to the highly conductive behavior of the CT complex. Such highly conductive Mott insulators, as a result of a small $U_{\text{eff}}/4t$ value, have been extensively studied in TTM-TTP-I₃,^[31] DMTSA-BF₄,^[32] and the spirobiphenalenyl system.^[3] In particular, the spirobiphenalenyl system has a similar electronic structure to **1b**⁺ (i.e., weak interactions between phenalenyl radical and cation moieties through acetylene or spiroconjugation).

Changes in Crystal and Electronic Structure at Low Temperature

Upon cooling the CT complex below 280 K , a steep increase in electroresistivity ρ was observed, and the sample entered a semiconductive state with an activation energy of 0.30 eV below 240 K . Drastic changes in optical conductivity were observed at around 270 K (Figure 8). The lowest-energy

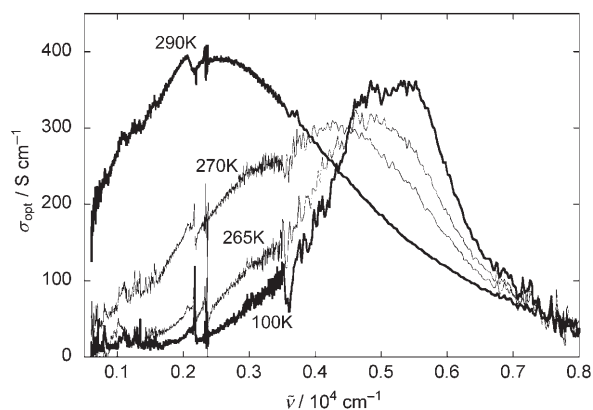


Figure 8. Variable-temperature optical conductivities σ_{opt} of **1b**-F₄-TCNQ obtained with light polarized along the *a* axis on the single-crystal (001) face.

band at 2600 cm^{-1} disappeared at 265 K , and a new higher-energy band appeared at around 5000 cm^{-1} . This new band was derived from isolated (i.e., monomeric) **1b**⁺, because the reaction of neutral **1b** with 1.1 equivalents of tris(4-bromophenyl)aminium hexachloroantimonate in CH_2Cl_2 at room temperature gave a low-energy intense band at 5550 cm^{-1} (see Supporting Information, Figure S5), which was assigned to a SOMO–LUMO transition of **1b**⁺ according to the INDO/S calculation.^[33] Thus, the semiconductive state at low temperature loses the delocalizing character of an electron in the π – π one-dimensional chain along the *a* axis, and the electron localizes on one **1b**⁺ molecule. X-ray crystallographic analysis at 90 K strongly supports this idea.^[34] At 90 K , σ bonds are formed between $\text{C}(\text{CN})_2$ of F₄-TCNQ and a phenalenyl carbon (C6 position in Figure 3). Figure 9 shows packing diagrams at room temperature and 90 K . The unit cell at 90 K is almost three times larger in volume than that at room temperature; thus, the cell should consist of three **1b** and three F₄-TCNQ fragments. Within the unit cell, two **1b** molecules react with one F₄-TCNQ

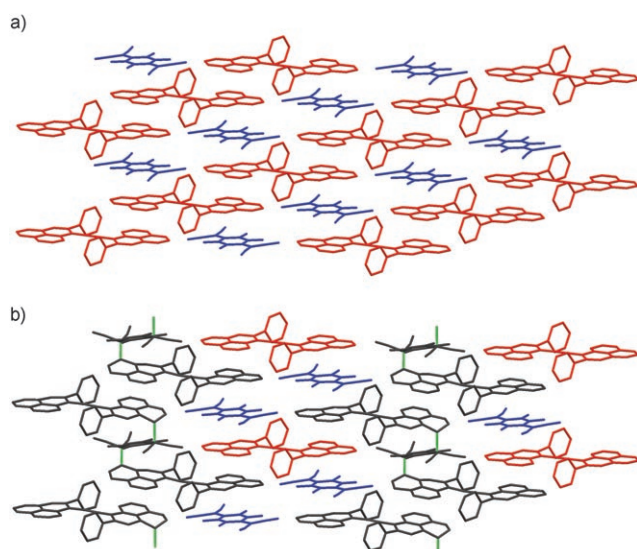


Figure 9. Crystal packing of **1b**-F₄-TCNQ at a) room temperature and b) 90 K. The green lines at 90 K represent the σ bonds formed between **1b** and F₄-TCNQ. The red molecules at 90 K are the radical-cation species **1b**⁺, each of which is crystallographically identical.

molecule, and one **1b** and two F₄-TCNQ molecules retain the original structure observed at room temperature. An unpaired electron localizes on the one **1b**⁺ molecule unchanged structurally, which is responsible for the higher-energy band at 5000 cm⁻¹ at low temperature. Notably, the optical and structural changes as a function of temperature are reversible.

Conclusions

We have prepared and characterized the bisphenalenyl system **1b** connected by acetylene, and confirmed its biradical character theoretically and experimentally. The two phenalenyl rings weakly perturbed by the acetylene linker are somewhat independent, which results in the small disproportionation energy ΔE of **1b**⁺ and the small on-site Coulombic repulsion U_{eff} in the CT complex of **1b** and F₄-TCNQ. The characteristic staggered stacking on the phenalenyl rings was established in the one-dimensional infinite chain of **1b**⁺ in the CT complex; consequently, a large transfer integral t was obtained. The electronic structure of the phenalenyl radical, which is characterized by the highly symmetric nonbonding SOMO, largely contributes to the small $U_{\text{eff}}/4t$ ratio and, accordingly, to the metallic-like conductive behavior at around room temperature in the CT complex. Unfortunately, the CT complex showed a steep increase in resistivity below 280 K due to σ -bond formation between **1b** and F₄-TCNQ. However, this bond formation would be suppressed by the exchange of F₄-TCNQ with inorganic counteranions such as BF₄⁻, ClO₄⁻, and SbCl₆⁻. Mott insulators have a strong correlation of electrons, which has attracted much interest over the decades not only in the

fundamental physical understanding of the metal–insulator transition^[35a] but also in the development of high- T_c superconductive materials.^[35b,c,d] Our study demonstrated that monocationic species of bisphenalenyl molecules might be promising compounds for highly conductive Mott insulators. Phenalenyl-based singlet biradicals have the characteristic feature of weakly coupled electrons together with potentially effective π – π overlap; this unusual electronic structure should play an important role in the rational search for new functional properties.

Experimental Section

General

All experiments with moisture- or air-sensitive compounds were performed in anhydrous solvents under argon atmosphere in well-dried glassware. Dried solvents were prepared by distillation under argon. Anhydrous ethanol was dried and distilled over Mg/I₂. THF was dried and distilled over sodium/benzophenone. Benzene, dichloromethane, toluene, and 1,2-dichloroethane were dried and distilled over calcium hydride. Column chromatography was performed with silica gel 60 (Merck). The products **5** and **7** were mixtures of diastereomers. The diastereomeric mixture of **5** was used for the following deprotection, and the individual isomers of the deprotected product **6** were isolated. The individual isomers of **7** were not isolated for further transformations because all the isomers could lead to the single compound **1b**. Infrared spectra were recorded on a JASCO FT/IR-660M spectrometer. Electronic spectra were recorded with a Shimadzu UV-3100PC spectrometer. ¹H NMR spectra were obtained on JEOL EX-270 and LAMBDA-500 spectrometers. Positive EI and FAB mass spectra were obtained by using Shimadzu QP-5000 and JEOL JMS SX-102 mass spectrometers. Polarized reflection spectra in the infrared and visible regions were observed by using two spectrometers combined with a microscope: Nicolet Magna 760 FTIR spectrometer (600–12000 cm⁻¹) and Atago Macs 320 multichannel detection system (11000–30000 cm⁻¹). The absolute reflectivity was determined by comparing the reflected light from a gold mirror and silicon single crystal, respectively. The single crystal was fixed with silicone grease on a copper sample holder, and the crystal face was adjusted to be normal to the incident light by use of the goniometer head. Low-temperature spectra were obtained by using an Oxford CF1104 helium-flow cryostat. Optical-conductivity spectra were calculated from the infrared reflection spectra with Kramers–Kronig analysis.^[36] Raman spectra were obtained with JASCO NR-1800 spectrometer. Four-probe direct-current resistance measurements were made on a single crystal, and electrical contacts to the crystal were made with a 25- μm gold wire and gold paint. Data collection for X-ray crystal analysis were performed on a Rigaku/MSM Mercury CCD diffractometer (MoK α , $\lambda = 0.71069 \text{ \AA}$). The structure was solved with direct methods and refined with full-matrix least squares (teXsan). Cyclic voltammetry was performed with a BAS CV-50W electrochemical analyzer. The cyclic voltammogram of **1b** ($5 \times 10^{-4} \text{ M}$) was recorded with a glassy carbon working electrode and a Pt counterelectrode in CH₂Cl₂ containing 0.1 M Bu₄NClO₄ as supporting electrolyte. The experiments employed an Ag/AgNO₃ reference electrode. Electrochemical experiments were done under nitrogen atmosphere at room temperature.

Computational Details

All DFT calculations were performed with the Gaussian 98 program.^[37] All geometry optimizations were carried out at the B3LYP level of theory with the 6-31G** basis set and C_{2v} symmetry constrains. Singlet-biradical character was estimated by using the CASSCF(2,2) method in RB3LYP-optimized geometry, and by using the broken-symmetry UB3LYP/6-31G** method along with geometry optimization. The band-structure calculation was performed with the extended HMO method by using the YAeHMOP package^[38] in X-ray crystallographic geometry. INDO/S calculations were conducted with the CAChe Ver. 4.5 software.

Syntheses

2: A solution of sodium ethoxide was freshly prepared from anhydrous ethanol (15 mL) and sodium (0.54 g, 23 mmol) in a 100-mL three-necked round-bottomed flask at room temperature. Diethyl phenylmalonate (5.0 mL, 23 mmol) was added to the colorless solution, and the mixture was stirred for 1 h under argon atmosphere. A solution of 1-chloromethyl-naphthalene (2.9 mL, 19 mmol) in ethanol (anhydrous, 10 mL) was added by cannula, and the reaction mixture was stirred overnight. Most of the ethanol was distilled off under reduced pressure, and the residue was mixed with water and ethyl acetate. The organic layer was separated, washed with aqueous NH_4Cl and brine, dried over Na_2SO_4 , and filtered. The filtrate was concentrated in vacuo. Recrystallization from hexane gave **2** (5.9 g, 83%) as colorless blocks. $R_f=0.43$ (benzene); m.p.: 84–85°C; IR (KBr): $\tilde{\nu}=1732, 1227\text{ cm}^{-1}$; $^1\text{H NMR}$ (270 MHz, CDCl_3): $\delta=1.16$ (t, $J=7.2$ Hz, 6H), 4.07–4.24 (m, 6H), 7.08–7.29 (m, 8H), 7.32–7.39 (m, 1H), 7.62 (d, $J=8.6$ Hz, 1H), 7.68 (d, $J=8.1$ Hz, 1H), 7.75 ppm (d, $J=7.9$ Hz, 1H); MS (EI): m/z (%) = 376 (2) $[M]^+$, 229 (9), 141 (100) $[M-\text{PhC}(\text{COOC}_2\text{H}_5)_2]^+$; elemental analysis: calcd (%) for $\text{C}_{24}\text{H}_{24}\text{O}_4$: C 76.57, H 6.43; found: C 76.57, H 6.42.

3: Ethyl ester **2** (5.9 g, 16 mmol) was suspended in ethanol (35 mL) in a 200-mL round-bottomed flask. A solution of potassium hydroxide (4.7 g, 84 mmol) in water (19 mL) was added to the suspension, and the mixture was heated under reflux at 90°C for 1 h. Most of the ethanol was distilled off, then aqueous HCl was added to acidify the solution, and the mixture was heated under reflux at 105°C for 1 h. The aqueous mixture was extracted repeatedly with diethyl ether. The combined organic layer was washed with brine, dried over Na_2SO_4 , and filtered. The solvent was removed in vacuo to give the colorless solid **3** (4.5 g). This material was used for the next reaction with no purification. $R_f=0.49$ (hexane/ethyl acetate = 1:1); $^1\text{H NMR}$ (270 MHz, CDCl_3): $\delta=3.47$ (dd, $J=6.3, 14.0$ Hz, 1H), 3.91 (dd, $J=8.3, 14.0$ Hz, 1H), 4.06 (dd, $J=6.3, 8.3$ Hz, 1H), 7.18 (d, $J=6.9$ Hz, 1H), 7.24–7.35 (m, 6H), 7.44–7.52 (m, 2H), 7.70 (d, $J=8.0$ Hz, 1H), 7.83–7.87 (m, 1H), 7.98–8.01 ppm (m, 1H).

4: A mixture of **3** (4.5 g, 16 mmol) and oxalyl chloride (40 mL) was heated at 82°C for 1 h in a 200-mL three-necked round-bottomed flask under argon atmosphere. After removal of excess oxalyl chloride under reduced pressure, the residue was dissolved in dichloromethane (50 mL), and the mixture was cooled to -78°C . Aluminum chloride (2.69 g, 20 mmol) was added to the cooled solution in one portion, and the reaction mixture was stirred for 2.5 h while being slowly warmed to -40°C . Aqueous HCl (3N) was added to the mixture, and the organic layer was separated. The aqueous layer was extracted with dichloromethane. The combined organic layer was washed with aqueous HCl (3N) and saturated aqueous NaHCO_3 , dried over Na_2SO_4 , and filtered. The solvent was removed in vacuo. After column chromatography on silica gel (benzene), **4** (2.5 g, 61%, 2 steps) was obtained as a pale-yellow solid. Further purification was done by recrystallization from benzene/hexane to give pale-yellow needles. $R_f=0.34$ (benzene); m.p.: 149–151°C; IR (KBr): $\tilde{\nu}=1680\text{ cm}^{-1}$; $^1\text{H NMR}$ (270 MHz, CDCl_3): $\delta=3.66$ –3.83 (m, 2H), 4.25 (dd, $J=6.6, 9.2$ Hz, 1H), 7.22–7.35 (m, 5H), 7.48–7.56 (m, 2H), 7.61 (dd, $J=7.2, 8.2$ Hz, 1H), 7.81–7.85 (m, 1H), 8.10 (dd, $J=1.3, 8.0$ Hz, 1H), 8.21 ppm (dd, $J=1.3, 7.2$ Hz, 1H); MS (EI): m/z (%) = 258 (100) $[M]^+$, 181 (34) $[M-\text{C}_6\text{H}_5]^+$; elemental analysis: calcd (%) for $\text{C}_{19}\text{H}_{14}\text{O}$: C 88.34, H 5.46; found: C 88.34, H 5.33.

5: *n*-Butyl lithium (1.6M in hexane, 4.9 mL, 7.8 mmol) was added slowly to a solution of bis(trimethylsilyl)acetylene (1.8 mL, 7.9 mmol) in THF (5.0 mL) at -78°C in a 50-mL Schlenk tube under argon atmosphere. The reaction mixture was warmed to room temperature and stirred for 2 h to generate lithium trimethylsilylacetylide. The reaction mixture was cooled to -78°C again, and a solution of **4** (1.0 g, 3.9 mmol) in THF (10 mL) was added dropwise by cannula. After 0.5 h (complete consumption of **4** was checked with TLC), dimethyl sulfate (1.3 mL, 14 mmol) was added, and the mixture was stirred for 9 h at room temperature. Water was added, and the mixture was stirred vigorously to hydrolyze the excess dimethyl sulfate. Diethyl ether was added to the mixture, and the organic layer was separated. The aqueous layer was extracted repeatedly with diethyl ether. The combined organic layer was washed with saturated aqueous NaHCO_3 and brine, dried over Na_2SO_4 , and filtered.

The solvent was removed in vacuo, and the residue was passed through a short pad of silica gel (hexane/ethyl acetate = 5:1 v/v) to give **5** as a colorless or pale-green oil (1.6 g, crude). This material was a mixture of two diastereomers (**5a** and **5b**) and was used for the next reaction without further purification. The two diastereomers could be separated for structural analysis by using repeated column chromatography on silica gel (hexane/ethyl acetate = 10:1). **5a**: $R_f=0.73$ (hexane/ethyl acetate = 4:1); $^1\text{H NMR}$ (270 MHz, CDCl_3): $\delta=0.08$ (s, 9H), 3.08 (s, 3H), 3.08–3.16 (m, 1H), 3.39–3.45 (m, 1H), 3.98–4.08 (m, 1H), 7.27–7.36 (m, 4H), 7.40–7.53 (m, 4H), 7.74 (d, $J=8.2$ Hz, 1H), 7.86 (dd, $J=0.6, 7.7$ Hz, 1H), 7.94 ppm (dd, $J=1.3, 7.1$ Hz, 1H); MS (EI): m/z (%) = 370 (6) $[M]^+$, 338 (47) $[M-\text{CH}_3\text{OH}]^+$, 265 (100). **5b**: $R_f=0.64$ (hexane/ethyl acetate = 4:1); $^1\text{H NMR}$ (270 MHz, CDCl_3): $\delta=0.12$ (s, 9H), 3.17 (s, 3H), 3.40 (dd, $J=4.1, 16.5$ Hz, 1H), 3.70–3.74 (m, 1H), 3.83 (dd, $J=5.9, 16.5$ Hz, 1H), 7.00–7.14 (m, 5H), 7.31–7.35 (m, 1H), 7.42–7.53 (m, 2H), 7.75 (d, $J=7.9$ Hz, 1H), 7.80 (dd, $J=1.2, 7.2$ Hz, 1H), 7.84 ppm (dd, $J=1.2, 8.2$ Hz, 1H); MS (EI): m/z (%) = 370 (9) $[M]^+$, 338 (44) $[M-\text{CH}_3\text{OH}]^+$, 265 (100).

6: TBAF (1.0M in THF, 4.0 mL, 4.0 mmol) was added to a solution of the diastereomeric mixture **5** (1.6 g, crude, 3.9 mmol) in THF (5 mL) in a 100-mL round-bottomed flask, and the mixture was stirred for 5 min at room temperature. After addition of aqueous NH_4Cl , the mixture was extracted repeatedly with diethyl ether. The combined organic layer was washed with brine, dried over Na_2SO_4 , and filtered. The filtrate was concentrated in vacuo. The residue was purified by column chromatography on silica gel (hexane/dichloromethane = 2:1 v/v). Two diastereomers, **6a** (colorless oil, 0.33 g, 28%) and **6b** (pale-yellow solid), were obtained. Compound **6a** included some impurities, which could not be removed by column chromatography or recrystallization. On the other hand, **6b** was purified by recrystallization from benzene/hexane to give colorless blocks (0.52 g, 43%). **6a**: $R_f=0.42$ (hexane/dichloromethane = 2:1); $^1\text{H NMR}$ (270 MHz, CDCl_3): $\delta=2.60$ (s, 1H), 3.12 (s, 3H), 3.13 (dd, $J=4.0, 16$ Hz, 1H), 3.45 (dd, $J=4.0, 13$ Hz, 1H), 3.95–4.06 (m, 1H), 7.30–7.57 (m, 8H), 7.76 (d, $J=8.1$ Hz, 1H), 7.88 (dd, $J=1.1, 8.3$ Hz, 1H), 7.96 ppm (dd, $J=1.2, 7.1$ Hz, 1H); MS (EI): m/z (%) = 298 (4) $[M]^+$, 266 (64) $[M-\text{CH}_3\text{OH}]^+$, 189 (100). **6b**: $R_f=0.29$ (hexane/dichloromethane = 2:1); m.p.: 150–151°C; IR (KBr): $\tilde{\nu}=3296, 2110\text{ cm}^{-1}$; $^1\text{H NMR}$ (270 MHz, CDCl_3): $\delta=2.69$ (s, 1H), 3.19 (s, 3H), 3.39 (dd, $J=4.4, 16$ Hz, 1H), 3.74–3.88 (m, 2H), 7.01–7.16 (m, 5H), 7.28–7.33 (m, 1H), 7.41–7.52 (m, 2H), 7.76 (d, $J=7.9$ Hz, 1H), 7.84–7.89 ppm (m, 2H); MS (EI): m/z (%) = 298 (7) $[M]^+$, 266 (64) $[M-\text{CH}_3\text{OH}]^+$, 189 (100); elemental analysis: calcd (%) for $\text{C}_{22}\text{H}_{18}\text{O}$: C 88.56, H 6.08; found: C 88.56, H 5.98.

7: EtMgBr (1.0M in THF, 1.2 mL, 1.2 mmol) was added to a solution of **6b** (0.3 g, 1.0 mmol) in THF (1.2 mL) in a 20-mL Schlenk tube, and the mixture was stirred for 0.5 h at room temperature under argon atmosphere. The reaction mixture was cooled to 0°C, and a solution of **4** (0.26 g, 1.0 mmol) in THF (2.8 mL) was added dropwise by cannula. The mixture was allowed to warm to room temperature and stirred for 1.5 h. After addition of aqueous NH_4Cl , the mixture was extracted repeatedly with diethyl ether. The combined organic layer was washed with brine, dried over Na_2SO_4 , and filtered. The filtrate was concentrated in vacuo. The residue was purified by column chromatography on silica gel (hexane/dichloromethane = 2:1–0:1 v/v) to give **7** (282 mg, 51%), which included three isomers (**7a**, **7b**, and **7c**). This diastereomeric mixture was used for the next reaction without further purification. However, each isomer could be separated for structural analysis by using repeated column chromatography on silica gel (hexane/dichloromethane = 1:1 v/v). **7a**: $R_f=0.27$ (hexane/ethyl acetate = 6:1); $^1\text{H NMR}$ (270 MHz, CDCl_3): $\delta=2.07$ (s, 1H), 2.87 (s, 3H), 3.11–3.25 (m, 2H), 3.40 (dd, $J=3.4, 13$ Hz, 1H), 3.65–3.71 (m, 2H), 3.82–3.92 (m, 1H), 6.90–6.94 (m, 2H), 7.02–7.16 (m, 3H), 7.22–7.32 (m, 6H), 7.36–7.49 (m, 7H), 7.71–7.85 ppm (m, 4H); MS (EI): m/z (%) = 556 (16) $[M]^+$, 152 (100). **7b**: $R_f=0.22$ (hexane/ethyl acetate = 6:1); $^1\text{H NMR}$ (270 MHz, CDCl_3): $\delta=2.45$ (s, 1H), 2.96 (s, 3H), 3.16–3.24 (m, 2H), 3.33 (dd, $J=3.6, 12$ Hz, 1H), 3.56–3.68 (m, 3H), 6.69–6.82 (m, 4H), 6.94–7.00 (m, 1H), 7.15–7.31 (m, 8H), 7.36–7.55 (m, 4H), 7.71 (d, $J=8.2$ Hz, 1H), 7.77–7.85 ppm (m, 4H); MS (EI): m/z (%) = 557 (12) $[M+\text{H}]^+$, 556 (10) $[M]^+$, 152 (100). **7c**: $R_f=0.17$ (hexane/ethyl acetate = 6:1); $^1\text{H NMR}$ (270 MHz, CDCl_3): $\delta=2.42$ (s, 1H), 2.99 (s, 3H), 2.97–3.12 (m, 2H), 3.18–3.36 (m, 2H), 3.43–3.48 (m, 2H), 6.51 (br d, $J=$

7.3 Hz, 2H), 6.77–6.83 (m, 2H), 6.93 (br d, $J=7.4$ Hz, 2H), 7.01–7.14 (m, 3H), 7.20–7.29 (m, 2H), 7.41–7.59 (m, 6H), 7.76–7.89 ppm (m, 5H); MS (EI): m/z (%) = 557 (12) $[M+H]^+$, 556 (11) $[M]^+$, 152 (100).

8: A solution of the diastereomeric mixture **7** (282 mg, 0.51 mmol) in benzene (10 mL) was heated under reflux at 95 °C under argon atmosphere in a 100-mL two-necked round-bottomed flask. TsOH·H₂O (5 mg, 0.03 mmol) was added to the solution, and the reaction mixture was heated under reflux for 5 min. The mixture was then cooled in an ice bath. The crude product was purified with flash column chromatography on silica gel (dichloromethane). The solvent was removed in vacuo, and the dehydrated compound **8** was obtained as an air-sensitive dark-grayish-violet powder (244 mg). $R_f=0.29$ (hexane/benzene=2:1); MS (EI): m/z (%) = 506 (16) $[M]^+$, 252 (100).

1b: A solution of **8** (244 mg, 0.48 mmol) in benzene (100 mL) was heated under reflux at 95 °C under argon atmosphere in a 200-mL round-bottomed flask. DDQ (120 mg, 0.53 mmol) was added to the solution, and the reaction mixture was heated under reflux for 10 min. The mixture was then cooled in an ice bath. The crude product was purified by column chromatography on silica gel (dichloromethane) to give **1b** (220 mg, 92%, 2 steps) as a dark-grayish-blue powder. Further purification was done by recrystallization from toluene to give dark-blue prisms. $R_f=0.32$ (hexane/benzene=2:1); m.p.: > 300 °C; Raman: 2014 cm⁻¹; ¹H NMR (500 MHz, CDCl₃): $\delta=6.59$ (d, $J=8.0$ Hz, 2H), 6.94 (s, 2H), 7.01 (t, $J=8.0$ Hz, 2H), 7.22 (d, $J=8.0$ Hz, 2H), 7.30 (t, $J=8.0$ Hz, 2H), 7.45–7.50 (m, 4H), 7.50–7.54 (m, 4H), 7.57–7.63 ppm (m, 6H); MS (EI): m/z (%) = 504 (5) $[M]^+$, 252 (100); elemental analysis: calcd (%) for C₄₀H₂₄: C 95.21, H 4.79; found: C 95.11, H 4.72.

CT complex of **1b** and F₄-TCNQ: Crystals of **1b** (1.5 mg, 3.0 × 10⁻³ mmol) and F₄-TCNQ (1.0 mg, 3.6 × 10⁻³ mmol) were placed at the bottom of each side of an H-shaped tube. Diffusion in toluene (10 mL) at 20 °C for about one week afforded the CT complex as black plates suitable for X-ray analysis. M.p.: > 300 °C; Raman: 2172, 1643 cm⁻¹; elemental analysis: calcd (%) for C₅₂H₂₄F₄N₄: C 79.99, H 3.10, N 7.18; found: C 80.30, H 3.25, N 6.89. Diffusion of **1b** and F₄-TCNQ in 1,2-dichloroethane (10 mL) at 20 °C also gave single crystals of the CT complex, which were used for polarized reflection spectroscopy and electroconductivity measurements. The crystals from toluene and 1,2-dichloroethane had the same crystal structures according to X-ray analysis.

Generation of **1b**⁺ for electronic absorption spectroscopy: A solution of tris(4-bromophenyl)ammonium hexachloroantimonate in CH₂Cl₂ (1.8 × 10⁻⁵ M, 2.2 mL) was added to a solution of **1b** in CH₂Cl₂ (1.8 × 10⁻⁵ M, 2 mL) at room temperature. The resulting pale-green solution was used to obtain the electronic absorption spectrum.

Acknowledgements

This work was partly supported by Grants-in-Aid for Scientific Research (No. 17550034 and 18350007) from the Japan Society for the Promotion of Science, a Grant-in-Aid for Scientific Research in Priority Areas "Application of Molecular Spins" (Area No. 769) from the Ministry of Education, Culture, Sports, Science, and Technology, Japan, and PRESTO-JST.

- [1] a) A. F. Garito, A. J. Heeger, *Acc. Chem. Res.* **1974**, *7*, 232–240; b) J. B. Torrance, *Acc. Chem. Res.* **1979**, *12*, 79–86.
 [2] a) G. Saito, Y. Yoshida, *Bull. Chem. Soc. Jpn.* **2007**, *80*, 1–137; b) V. Khodorokovsky, J. Y. Becker in *Organic Conductors: Fundamentals and Applications* (Ed.: J.-P. Farges), Marcel Dekker, New York, **1994**, pp. 75–114; c) M. Bendikov, F. Wudl, D. F. Perepichka, *Chem. Rev.* **2004**, *104*, 4891–4945; d) *TTF Chemistry: Fundamentals and Applications of Tetrathiafulvalene* (Eds.: J. Yamada, T. Sugimoto), Kodansha & Springer, Tokyo, **2004**.
 [3] a) X. Chi, M. E. Itkis, B. O. Patrick, T. M. Barclay, R. W. Reed, R. T. Oakley, A. W. Cordes, R. C. Haddon, *J. Am. Chem. Soc.* **1999**, *121*,

- 10395–10402; b) S. K. Pal, M. E. Itkis, F. S. Tham, R. W. Reed, R. T. Oakley, R. C. Haddon, *Science* **2005**, *309*, 281–284.
 [4] a) D. H. Reid, *Q. Rev. Chem. Soc.* **1965**, *19*, 274–302; b) R. C. Haddon, *Nature* **1975**, *256*, 394–396.
 [5] Our recent work on the phenalenyl system: a) Y. Morita, T. Aoki, K. Fukui, S. Nakazawa, K. Tamaki, S. Suzuki, A. Fuyuhiko, K. Yamamoto, K. Sato, D. Shiomi, A. Naito, T. Takui, K. Nakasuji, *Angew. Chem.* **2002**, *114*, 1871–1874; *Angew. Chem. Int. Ed.* **2002**, *41*, 1793–1796; b) S. Nishida, Y. Morita, K. Fukui, K. Sato, D. Shiomi, T. Takui, K. Nakasuji, *Angew. Chem.* **2005**, *117*, 7443–7446; *Angew. Chem. Int. Ed.* **2005**, *44*, 7277–7280; c) S. Suzuki, Y. Morita, K. Fukui, K. Sato, D. Shiomi, T. Takui, K. Nakasuji, *J. Am. Chem. Soc.* **2006**, *128*, 2530–2531; d) T. Murata, Y. Morita, K. Fukui, K. Tamaki, H. Yamochi, G. Saito, K. Nakasuji, *Bull. Chem. Soc. Jpn.* **2006**, *79*, 894–913.
 [6] R. C. Haddon, F. Wudl, M. L. Kaplan, J. H. Marshall, R. E. Cais, F. B. Bramwell, *J. Am. Chem. Soc.* **1978**, *100*, 7629–7633.
 [7] R. T. Boere, K. H. Moock, *J. Am. Chem. Soc.* **1995**, *117*, 4755–4760.
 [8] K. Goto, T. Kubo, K. Yamamoto, K. Nakasuji, K. Sato, D. Shiomi, T. Takui, M. Kubota, T. Kobayashi, K. Yakushi, J. Ouyang, *J. Am. Chem. Soc.* **1999**, *121*, 1619–1620.
 [9] a) T. Kubo, M. Sakamoto, M. Akabane, Y. Fujiwara, K. Yamamoto, M. Akita, K. Inoue, T. Takui, K. Nakasuji, *Angew. Chem.* **2004**, *116*, 6636–6641; *Angew. Chem. Int. Ed.* **2004**, *43*, 6474–6479; b) T. Kubo, A. Shimizu, M. Sakamoto, M. Uruichi, K. Yakushi, M. Nakano, D. Shiomi, K. Sato, T. Takui, Y. Morita, K. Nakasuji, *Angew. Chem.* **2005**, *117*, 6722–6726; *Angew. Chem. Int. Ed.* **2005**, *44*, 6564–6568; c) T. Kubo, A. Shimizu, M. Uruichi, K. Yakushi, M. Nakano, D. Shiomi, K. Sato, T. Takui, Y. Morita, K. Nakasuji, *Org. Lett.* **2007**, *9*, 81–84.
 [10] M. S. Platz in *Diradicals* (Ed.: W. T. Borden), Wiley, New York, **1982**, pp. 195–258; recent work in organic biradicaloids: a) D. R. McMasters, J. Wirz, *J. Am. Chem. Soc.* **2001**, *123*, 238–246; b) A. Kikuchi, F. Iwahori, J. Abe, *J. Am. Chem. Soc.* **2004**, *126*, 6526–6527; c) M. Bendikov, H. M. Duong, K. Starkey, K. N. Houk, E. A. Carter, F. Wudl, *J. Am. Chem. Soc.* **2004**, *126*, 7416–7417; d) R. Ziessel, C. Stroh, H. Heise, F. H. Köhler, P. Turek, N. Claiser, M. Souhassou, C. Lecomte, *J. Am. Chem. Soc.* **2004**, *126*, 12604–12613.
 [11] J. Huang, M. Kertesz, *J. Am. Chem. Soc.* **2007**, *129*, 1634–1643.
 [12] D. Small, V. Zaitsev, Y. Jung, S. V. Rosokha, M. Head-Gordon, J. K. Kochi, *J. Am. Chem. Soc.* **2004**, *126*, 13850–13858.
 [13] K. Nakasuji, K. Yoshida, I. Murata, *Chem. Lett.* **1982**, 969–970.
 [14] W. P. Purcell, J. A. Singer, *J. Chem. Eng. Data* **1967**, *12*, 235–246.
 [15] a) D. Döhnert, J. Koutecký, *J. Am. Chem. Soc.* **1980**, *102*, 1789–1796; b) Y. Jung, M. Head-Gordon, *ChemPhysChem* **2003**, *4*, 522–525.
 [16] V. Bonačić-Koutecký, J. Koutecký, J. Michl, *Angew. Chem.* **1987**, *99*, 216–236; *Angew. Chem. Int. Ed.* **1987**, *26*, 170–189.
 [17] a) V. Bachler, G. Olbrich, F. Neese, K. Wieghardt, *Inorg. Chem.* **2002**, *41*, 4179–4193; b) D. Herebian, K. E. Wieghardt, F. Neese, *J. Am. Chem. Soc.* **2003**, *125*, 10997–11005.
 [18] The electrochemical HOMO–LUMO gap of **1b** is slightly different from that of **1a** reported in reference [13], presumably due to irreversibility of the redox waves of **1a**.
 [19] R. Hoffmann, *J. Am. Chem. Soc.* **1968**, *90*, 1475–1485.
 [20] The theoretical singlet–triplet energy gap for **1a** calculated by the UB3LYP/6–31G** method was 35.8 kJ mol⁻¹ (= 4300 K), from which the amount of triplet species at 400 K was estimated to be about 0.01% according to the Boltzmann distribution. Accordingly, ESR signals typical for triplet species could not be detected in the solid **1b**. On the other hand, the appearance of NMR signals is more sensitive to paramagnetic species, as it is well-known that these species greatly decrease spin–lattice relaxation times T_1 . Even very small amounts of paramagnetic species can influence the linewidth of signals and cause signal broadening in NMR spectra.
 [21] Crystal data for **1b**: triclinic, $P\bar{1}$ (No. 2), $a=5.681(2)$, $b=9.368(5)$, $c=12.688(6)$ Å, $\alpha=80.75(2)$, $\beta=75.68(2)$, $\gamma=77.86(2)^\circ$, $V=635.4(5)$ Å³, $Z=1$, $R1$ ($wR2$)=0.069 (0.208) for 181 parameters and 1730 unique reflections with $I>2\sigma(I)$, GOF=1.10. CCDC-296369

- contains the supplementary crystallographic data for this paper. These data can be obtained free of charge from The Cambridge Crystallographic Data Centre at http://www.ccdc.cam.ac.uk/data_request/cif.
- [22] C. P. Brock, J. D. Dunitz, *Acta Crystallogr. Sect. B* **1982**, *38*, 2218–2228.
- [23] a) E. Weber, W. Seichter, R. J. Wang, T. C. W. Mak, *Bull. Chem. Soc. Jpn.* **1991**, *64*, 659–667; b) Z. Berkovitch-Yellin, L. Leiserowitz, *Acta Crystallogr. Sect. B* **1977**, *33*, 3657–3669; c) G. Dyker, S. Borowski, G. Henkel, A. Kellner, I. Dix, P. G. Jones, *Tetrahedron Lett.* **2000**, *41*, 8259–8262. For standard C(sp)–C(sp), C(sp)–C(sp²), and C(sp²)–C(sp²) bond lengths, see: O. Bastiansen, M. Trätteberg, *Tetrahedron* **1962**, *17*, 147–154.
- [24] P. Kaszynski, *J. Phys. Chem. A* **2001**, *105*, 7626–7633.
- [25] a) W. Sümmerrmann, G. Kothe, H. Baumgärtel, H. Zimmermann, *Tetrahedron Lett.* **1969**, *10*, 3807–3810; b) S. Utamapanya, A. Rajca, *J. Am. Chem. Soc.* **1991**, *113*, 9242–9251; see also: G.-L. Xu, G. Zou, Y.-H. Ni, M. C. DeRosa, R. J. Crutchley, T. Ren, *J. Am. Chem. Soc.* **2003**, *125*, 10057–10065.
- [26] M. Meneghetti, C. Pecile, *J. Chem. Phys.* **1986**, *84*, 4149–4162.
- [27] F. Gerson, J. Knöbel, A. Metzger, I. Murata, K. Nakasuji, *Helv. Chim. Acta* **1984**, *67*, 934–938.
- [28] Crystal data for **1b**-F₄-TCNQ at room temperature: triclinic, *P* $\bar{1}$ (No. 2), *a* = 9.1553(0), *b* = 10.3356(5), *c* = 11.4109(2) Å, α = 65.55(2), β = 76.74(2), γ = 70.63(2)°, *V* = 921.9(2) Å³, *Z* = 1, *R1* (*wR2*) = 0.056 (0.164) for 271 parameters and 2024 unique reflections with *I* > 2σ(*I*), GOF = 1.116. CCDC-640749 contains the supplementary crystallographic data for this paper.
- [29] The *U*_{eff} and *t* values were determined by a general procedure with the following parameters: *E*_{ca} = 0.32 eV, *f* = 0.70, *d* = 9.155 × 10⁻¹⁰ m; see: a) M. Yoshitake, K. Yakushi, H. Kuroda, A. Kobayashi, R. Kato, H. Kobayashi, *Bull. Chem. Soc. Jpn.* **1988**, *61*, 1115–1119; b) C. S. Jacobsen in *Highly Conducting Quasi-One-Dimensional Organic Crystals, Semiconductors and Semimetals Series Vol. 27* (Ed.: E. Conwell), Academic Press, New York, **1988**, pp. 293–384; c) K. Yakushi, *Bull. Chem. Soc. Jpn.* **2000**, *73*, 2643–2662.
- [30] A molecule with completely independent redox centers would show redox waves with small separations of (2*RT/F*)ln*k* for the first and *k*th electron transfers; see reference [25b].
- [31] T. Mori, H. Inokuchi, Y. Misaki, T. Yamabe, H. Mori, S. Tanaka, *Bull. Chem. Soc. Jpn.* **1994**, *67*, 661–667.
- [32] a) K. Takimiya, A. Ohnishi, Y. Aso, T. Otsubo, F. Ogura, K. Kawabata, K. Tanaka, M. Mizutani, *Bull. Chem. Soc. Jpn.* **1994**, *67*, 766–772; b) J. Dong, K. Yakushi, K. Takimiya, T. Otsubo, *J. Phys. Soc. Jpn.* **1998**, *67*, 971–977.
- [33] An ROHF INDO/S calculation for **1b**^{•+} predicted a symmetry-allowed SOMO–LUMO transition at 6290 cm⁻¹ (*f* = 0.33).
- [34] Crystal data for **1b**-F₄-TCNQ at 90 K: triclinic, *P1* (No. 1), *a* = 10.135(3), *b* = 12.694(3), *c* = 21.151(8) Å, α = 83.09(1), β = 89.87(1), γ = 83.73(3)°, *V* = 2685(1) Å³, *Z* = 3, *R1* (*wR2*) = 0.118 (0.245) for 1621 parameters and 6479 unique reflections with *I* > 2σ(*I*), GOF = 1.616. Notably, bond lengths and angles include uncertainty associated with the high *R1* value.
- [35] a) M. Imada, A. Fujimori, Y. Tokura, *Rev. Mod. Phys.* **1998**, *70*, 1039–1263; b) P. W. Anderson, *Science* **1987**, *235*, 1196–1198; c) S. A. Kivelson, V. J. Emery, *Synth. Met.* **1996**, *80*, 151–158; d) T. Giamarchi, *Chem. Rev.* **2004**, *104*, 5037–5055.
- [36] R. K. Ahrenkiel, *J. Opt. Soc. Am.* **1971**, *61*, 1651–1655.
- [37] M. J. Frisch, G. W. Trucks, H. B. Schlegel, G. E. Scuseria, M. A. Robb, J. R. Cheeseman, V. G. Zakrzewski, J. A. Montgomery, Jr., R. E. Stratmann, J. C. Burant, S. Dapprich, J. M. Millam, A. D. Daniels, K. N. Kudin, M. C. Strain, O. Farkas, J. Tomasi, V. Barone, M. Cossi, R. Cammi, B. Mennucci, C. Pomelli, C. Adamo, S. Clifford, J. Ochterski, G. A. Petersson, P. Y. Ayala, Q. Cui, K. Morokuma, D. K. Malick, A. D. Rabuck, K. Raghavachari, J. B. Foresman, J. Cioslowski, J. V. Ortiz, A. G. Baboul, B. B. Stefanov, G. Liu, A. Liashenko, P. Piskorz, I. Komaromi, R. Gomperts, R. L. Martin, D. J. Fox, T. Keith, M. A. Al-Laham, C. Y. Peng, A. Nanayakkara, C. Gonzalez, M. Challacombe, P. M. W. Gill, B. G. Johnson, W. Chen, M. W. Wong, J. L. Andres, M. Head-Gordon, E. S. Replogle, J. A. Pople, Gaussian 98 (Revision A11.3), Gaussian, Inc., Pittsburgh, PA (USA), **1998**.
- [38] G. A. Landrum, W. V. Glassey, “Yet Another Extended Hückel Molecular Orbital Package (YAeHMOP, including Bind 3.0 and Viewkel 3.0)”, to be found under <http://sourceforge.net/projects/yaehmop/>, **2001**.

Received: April 23, 2007
 Published online: September 7, 2007